Tensile Loading of Ropes of Single Wall Carbon Nanotubes and their Mechanical Properties

Min-Feng Yu,[1] Bradley S. Files,[2] Sivaram Arepalli,[3] and Rodney S. Ruoff[1,*]
[1]*Department of Physics, Washington University–St. Louis, St. Louis, Missouri 63130*
[2]*EM2—Materials and Process Technology Branch, NASA/Johnson Space Center, Houston, Texas 77058*
[3]*G_B_Tech/Lockheed Martin, 2400 NASA Road One, Houston, Texas 77058*
(Received 26 January 2000)

The mechanical response of 15 single wall carbon nanotube (SWCNT) ropes under tensile load was measured. For 8 of these ropes strain data were obtained and they broke at strain values of 5.3% or lower. The force-strain data are well fit by a model that assumes the load is carried by the SWCNTs on the perimeter of each rope. This model provides an average breaking strength of SWCNTs on the perimeter of each rope; the 15 values range from 13 to 52 GPa (mean 30 GPa). Based on the same model the 8 average Young's modulus values determined range from 320 to 1470 GPa (mean 1002 GPa).

PACS numbers: 62.20.Fe, 61.48.+c, 81.40.Jj

Since their discovery [1,2], single wall carbon nanotubes (SWCNTs) have stimulated intense study. Unique electrical properties have been measured [3–5], and extraordinary mechanical performance projected from theoretical modeling [6–10]. SWCNTs are predicted to have extremely high Young's modulus values, similar to that of graphite in-plane (~1000 GPa) [11]. It is also predicted that SWCNTs can sustain large strain in the axial direction, and preferred strain-releasing mechanisms have been recently analyzed [6,8,9,12]. High breaking strengths are thus predicted for SWCNTs, generating interest for high strength, lightweight material applications. A recent model shows that a strained SWCNT can readily release strain energy by defect nucleation beyond a critical tensile strain of about 5% [6,8]. In contrast to the extensive theoretical modeling, there have been few experimental studies on the mechanical properties of SWCNTs [13–16], and no direct strength measurements prior to the work reported here.

Here, we extend the method previously used to measure the strength of individual multiwalled carbon nanotubes (MWCNT) [17,18] to SWCNT ropes. SWCNT ropes were tensile loaded in a "nanostressing stage" operated inside a LEO 1530 scanning electron microscope (SEM). The SWCNT sample used in the experiment was made by the laser ablation method and purified by refluxing and filtration [19]. We tore the resulting SWCNT "paper" apart, which caused individual SWCNT ropes to project from the tear edge. In our previous work we mounted individual MWCNTs across opposing atomic force microscope (AFM) tips, followed by application of tensile load [18]. However, this has been extremely difficult to do for the SWCNT ropes. Each rope was too tightly entangled with other ropes to be teased away from the bulk sample without breaking it; consequently, we modified the previous nanostressing stage. Here, a parallel bimorph (a piezo actuator made of bonded piezo films) was added onto the stage [20], and used as a flexure element to provide the force and displacement needed. An AFM probe (with cantilevers having force constants of about 0.4 N/m) [21] is then attached onto the bimorph [Fig. 1(e)]. The bimorph can provide a deflection of up to 150 μm and a force up to 0.1 N. The sharp point at the AFM tip facilitates the attachment of individual SWCNT ropes projecting out of the SWCNT paper using the same method of electron beam-induced decomposition of residual hydrocarbons as previously described [18]. The AFM probe also acts as the force sensor to read out the applied load. The whole tensile-loading experiment is recorded on video via the video output of the SEM. Figure 1 shows SEM images of a SWCNT rope, including the deposit forming the SWCNT attachment of the free rope end to the AFM tip surface, before and after the nanotube broke due to the application of tensile load.

A schematic describing how the force and the strain in the SWCNT rope are measured is shown in Fig. 1(e). First, the dependence of the deflection S of the AFM tip as a function of applied voltage to the bimorph was independently determined in the absence of any attached specimen. Second, while the SWCNT rope is being stretched due to application of a given voltage to the bimorph, the AFM tip position change, S', is directly recorded in a slow-scan mode image. The true deflection of the AFM cantilever is $S - S'$. The force constant of the cantilever multiplied by its deflection gives the tensile force applied to the SWCNT rope. Calibration of S allowed much higher magnification imaging of just the enclosed region in Fig. 1(e), yielding more accurate determination of length changes in the rope (and thus the strain). The other end of the SWCNT rope in contact with the SWCNT paper was entangled with other ropes, so it was difficult to define precisely an end position to determine the specimen length. Fortunately, internal marks were often present, in the form of small particles attached along the loaded rope section. It was possible to use such marks for 8 of the 15 SWCNT ropes; the length change between these marks, δL, as a function of applied load was measured and the strain, $\delta L/L$ [Fig. 1(e)], thereby obtained [22].

Finally, there are the questions of what the cross-sectional shape of the SWCNT rope was, and which SWCNTs in the rope were initially carrying the load. SWCNT ropes consist of a close-packed array of

 0031-9007/00/84(24)/5552(4)$15.00

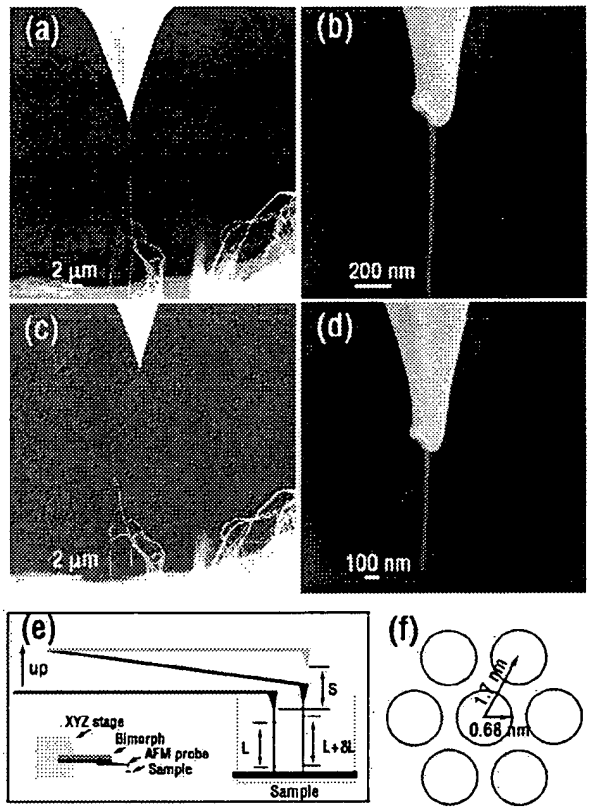

FIG. 1. SEM images showing a SWCNT rope tensile-loading experiment, before and after the SWCNT rope was broken. (a) A tensile loaded SWCNT rope between an AFM tip and a SWCNT "paper" sample. (b) Close-up view showing the attachment (carbonaceous deposit) of the end of the SWCNT rope to the AFM tip. (c) The same SWCNT rope after being loaded to the point where it broke. The image shows that one rope fragment was about 1 μm from the attachment region on the AFM tip. (d) Another close-up view of the attachment area after the rope was broken, showing the deposit was still robust. (e) A schematic showing an overview of the tensile-loading experiment. In the schematic, the gray cantilever indicates where the cantilever would be if no rope were attached on the AFM tip. (f) The assumed close-packed SWCNT rope with hexagonal cross section used in the paper for the purpose of calculating the cross-sectional area from the diameter measured with the SEM.

SWCNTs [23–25]. We assume that all SWCNTs in the ropes studied here are (10, 10) nanotubes, with a diameter of 1.36 nm [Fig. 1(f)]. TEM and SEM observations of the SWCNT paper sample show that rope cross sections are generally round in shape.

Two separate treatments for calculating the cross-sectional area to be used for determining the applied stress give low-end and high-end values for the breaking strength and Young's modulus values of these SWCNT ropes. In the first treatment, every SWCNT in the rope is assumed to carry an equal load. Then, the cross-sectional area is defined as the total number of SWCNTs [26] in the rope multiplied by the cross-sectional area of a SWCNT (πtd, where t is the SWCNT wall thickness, 0.34 nm, and d is the SWCNT diameter, assumed to be 1.36 nm). In the second treatment, only the perimeter SWCNTs in the close-packed SWCNT rope are assumed to carry the initial load, so the load-bearing cross-sectional area is equal to the total number of SWCNTs [26] on the perimeter of the rope multiplied by the cross-sectional area of a SWCNT. We thus obtained two sets of average strength and Young's modulus values for the SWCNTs in these ropes. The 8 average Young's modulus values were obtained by a linear fit of each stress-strain curve for the 8 ropes for which strain could be measured. Figure 2 shows the stress-strain curves with stress calculated from the "perimeter" model. (The general trend of the curves will be the same for the case of the stress calculated using the full cross-sectional area.) The average breaking strength value, σ_p, and average Young's modulus value, E_p, of the perimeter SWCNTs for each rope are shown in Table I. These average strength values range from 13 to 52 GPa, and the average Young's modulus values range from 320 to 1470 GPa. A comparison with our work on MWCNTs where the outer shell was proven to be carrying the load is relevant. The 19 MWCNT (outer shell) strength values ranged from 11 to 63 GPa and the four MWCNT Young's modulus values determined ranged from 270 to 950 GPa [18]. Carbon fibers have been previously measured to have E values as high as 900 GPa [27]. For the SWCNT ropes studied here, there does not appear to be any obvious dependence of strength (σ_p) or modulus (E_p) on the rope diameter. It is found that σ_p is weakly proportional to E_p. In contrast, there is typically an inverse dependence

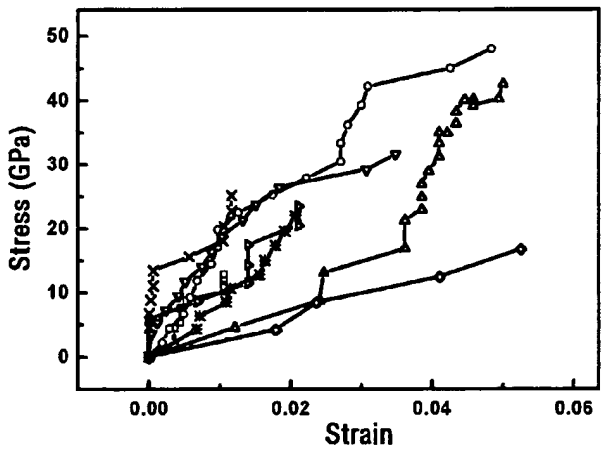

FIG. 2. Eight stress versus strain curves obtained from the tensile-loading experiments on individual SWCNT ropes. Each rope diameter is measured at high magnification (~100 000) in the SEM, accuracy a few nm. The stress values have been calculated using the cross-sectional area of the perimeter SWCNTs, according to the geometric model [see Fig. 1(f) and Ref. [23]). The SWCNT ropes for which strain could be determined were (see also Table I) C (□), D (○), E (△), G (▽), K (◇), M (▷), O (*), P (×).

TABLE I. List of the SWCNT ropes measured in the tensile-loading experiment. Shown are the rope sample, the diameter D of the rope, the breaking strain ε (percent value), the breaking strength σ_e and the Young's modulus E_e considering all SWCNTs in the rope to be carrying the applied load, and the breaking strength σ_p and the Young's modulus E_p calculated considering only SWCNTs in the perimeter of the rope to be carrying the applied load. The ellipses in the table indicate that values were not obtained.

Sample	D (nm)	ε (%)	σ_e (GPa)	E_e (GPa)	σ_p (GPa)	E_p (GPa)
A	20	...	11	...	33	...
B	40	...	9	...	52	...
C	21	1.1	4	315	13	1070
D	38	4.8	8	180	48	1040
E	35	5.0	8	270	43	1470
F	27	...	11	...	45	...
G	39	3.5	5	140	32	860
H	34	...	3	...	16	...
I	41	...	6	...	37	...
K	23	5.3	5	91	17	320
L	34	...	5	...	29	...
M	23	2.1	7	250	23	880
N	23	...	4	...	15	...
O	19	2.1	7	350	22	1050
P	23	1.2	7	380	25	1330

between strength and modulus for carbon fibers [27]. For the 8 ropes where strain could be measured there is no obvious dependence of strain on either E_p or σ_p.

Also in Table I are values for the average breaking strength, σ_e, and average Young's modulus, E_e, with the assumption that all SWCNTs in the rope participate equally in carrying the load. A comparison of σ_e and σ_p shows that to achieve extremely high engineering modulus and strength values in applications using SWCNT ropes where the perimeter SWCNTs are actually carrying the load, ropes should probably contain about 10 SWCNTs or less. This maximizes the number of perimeter SWCNTs relative to interior SWCNTs. This may explain the limited strength enhancement of some of the composites that have been tested at NASA/Johnson Space Center that have used relatively large diameter SWCNT ropes, similar to those studied here.

The second treatment (the perimeter model) is supported by further evidence as explained below. Figures 3(a) and 3(b) show the fragments left on the AFM tip and on the SWCNT paper from a SWCNT rope loading experiment, following breakage. As indicated by the arrows, there is an abrupt diameter change along each SWCNT rope fragment. The diameter change indicates that not all of the SWCNTs in the rope carried the initial tensile load and consequently did not break simultaneously or at the same location. As mentioned, the SWCNT rope is attached to the AFM tip by depositing carbonaceous material, which means that only the perimeter SWCNTs are in close contact with the deposit.

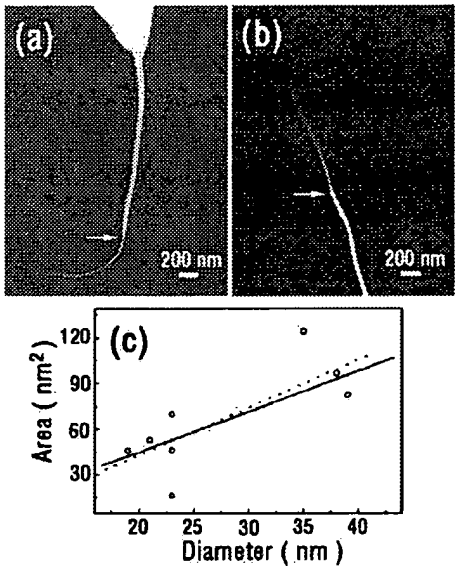

FIG. 3. SEM images (a) and (b) show the two fragments from one broken SWCNT rope, one left on the AFM tip and the other projecting from the SWCNT "paper" sample. Clear diameter changes are seen in these images and are indicated by arrows. (c) A plot of both the cross-sectional area A obtained from the fitting model (open circles) and the area A' calculated from the purely geometric model represented in Fig. 1(f) (dark line; see also Ref. [26]) vs the rope diameter. The dotted line is the best linear fit to the open circles.

In addition to the evidence from SEM images of SWCNT fragments, the cross-sectional area carrying the load can be estimated with a method commonly used in the mechanical measurement of fibers and whiskers. In this method, the cross-sectional area A is related to the load F as $A = F/(E\varepsilon)$ [28]. The product values of A and E can be directly obtained from the slope of the linear fit to each of 8 force versus strain curves. The dependence of the obtained values of the product of A and E (or A, since E can be assumed to be constant) on the diameter (D) values of the ropes can then help to determine the breaking mechanism. If all of the SWCNTs in the rope carried the load, then A would be proportional to the number of SWCNTs in the rope and thus to D^2. If only the perimeter SWCNTs carried the load, A would be linearly proportional to D. From the analysis of the product values of A and E, A is found to be significantly closer to being linearly dependent on D than on D^2. This linear dependence is seen as the dotted line in Fig. 3(c). The values of A are thus compared with the values of A' calculated from the geometry of the rope as follows. The lattice constant of the close-packed SWCNT rope is 1.7 nm [25]. By arranging the close-packed SWCNTs to fill a hexagonal cross section as shown in Fig. 1(f), the number of SWCNTs on the perimeter and thus their total cross-sectional area A' can be obtained for different rope diameters as measured with the SEM [26]. Figure 3(c) shows the comparison between the A' and A values so

obtained after assigning E to be 1000 GPa. The linear dependence of the A values on D obtained from the fitting approach described is very close to the A' vs D dependence calculated by assuming that only the perimeter SWCNTs in the close-packed SWCNT rope are carrying the load. Note that it is the close match of the slopes of the two plots in Fig. 3(c) that is most important in supporting the perimeter model.

The model that treats the perimeter SWCNTs in the ropes as the load-carrying elements supports the theoretical prediction that SWCNTs will have large Young's modulus and breaking strength values. The maximum breaking strain of 5.3% is close to the critical strain for defect nucleation of ~5% for individual SWCNTs based on theoretical simulation [12]. Here, we have studied the mechanical response of SWCNT ropes, and obtained the averaged mechanical properties of individual SWCNTs in these ropes from the models used, rather than tensile loading them individually. The mean value for the average breaking strength and the mean value for the average Young's modulus, Table I, for the model treating the perimeter SWCNTs as carrying the load, are 30 and 1002 GPa, respectively.

We acknowledge partial support for this work by ONR and DARPA, the NSF, and Zyvex. We thank O. Lourie and K. Ausman for support, and thank the staff at the Materials Science Center at the University of Wisconsin (UW) for their assistance. The NSF-Material Research and Science Engineering Center at UW provides support for the UW electron microscope facilities. We acknowledge W. Buhro, M. Dyer, A. Ruoff, and T. Kowalewski for critically reading the manuscript.

*To whom correspondence should be addressed.
Electronic addresses: ruoff@wuphys.wustl.edu, r_ruoff@northwestern.edu (after 1 September 2000).

[1] S. Iijima and T. Ichihashi, Nature (London) **363**, 603 (1993).
[2] D. S. Bethune *et al.*, Nature (London) **363**, 605 (1993).
[3] S. J. Tans *et al.*, Nature (London) **386**, 474 (1997).
[4] S. J. Tans, A. R. M. Verschueren, and C. Dekker, Nature (London) **393**, 49 (1998).
[5] T. W. Odom *et al.*, Nature (London) **391**, 62 (1998).
[6] B. I. Yakobson, in *Recent Advances in the Chemistry and Physics of Fullerences and Related Materials, Electrochemical Society,* edited by R. S. Ruoff and K. M. Kadish (Electrochemical Society, Inc., Pennington, NJ, 1997), Vol. 5 (97-42), p. 549.
[7] J. P. Lu, Phys. Rev. Lett. **79**, 1297 (1997).
[8] B. I. Yakobson, Appl. Phys. Lett. **72**, 918 (1998).
[9] M. Buongiorno Nardelli, B. I. Yakobson, and J. Bernholc, Phys. Rev. B **57**, R4277 (1998).
[10] E. Hernandez *et al.*, Phys. Rev. Lett. **80**, 4502 (1998).
[11] B. T. Kelly, *Physics of Graphite* (Applied Science, London, 1981).
[12] M. B. Nardelli, B. I. Yakobson, and J. Bernholc, Phys. Rev. Lett. **81**, 4780 (1998).
[13] A. Krishnan *et al.*, Phys. Rev. B **58**, 14031 (1998).
[14] J.-P. Salvetat *et al.*, Phys. Rev. Lett. **82**, 944 (1999).
[15] D. A. Walters *et al.*, Appl. Phys. Lett. **74**, 3803 (1999).
[16] J. R. Wood *et al.*, J. Phys. Chem. B **103**, 10388 (1999).
[17] M.-F. Yu *et al.*, Nanotechnology **10**, 244 (1999).
[18] M.-F. Yu *et al.*, Science **287**, 637 (2000).
[19] A. G. Rinzler *et al.*, Appl. Phys. A **67**, 29 (1998).
[20] Part Number: BIMP15/6/0.6-PX5-N, American Piezo Ceramics, Inc.
[21] Noncontact SC12 silicon cantilever, Silicon-Molecular Devices and Tools Ltd. The force constant of the cantilever is calibrated using its dimensions measured in SEM. In addition, the force constants of the 15 cantilevers used here were independently measured using calibrated AFM cantilevers from Thermomicroscopes. The average measured value differed by 7% from the average value calculated from the SEM determined geometry.
[22] J. J. Petrovic *et al.*, J. Mater. Sci. **20**, 1167 (1985).
[23] R. S. Ruoff *et al.*, Nature (London) **364**, 514 (1993).
[24] J. Tersoff and R. S. Ruoff, Phys. Rev. Lett. **73**, 676 (1994).
[25] A. Thess *et al.*, Science **273**, 483 (1996).
[26] The total number (N_p) of perimeter SWCNTs, and total number (N) of SWCNTs, in a SWCNT rope are calculated as follows. First, the number of SWCNTs across the diameter D (in nm) of the rope is defined as the least integer of $N_c = D/1.7$, where 1.7 is the lattice constant of a close-packed SWCNT rope. Then according to a simple geometric treatment, $N = (3N_c^2 + 1)/4$ and $N_p = 3(N_c - 1)$ for N_c odd, and $N = (3N_c^2 + 2N_c)/4$ and $N_p = 3N_c - 2$ for N_c even.
[27] M. S. Dresselhaus *et al.*, *Graphite Fibers and Filaments* (Springer-Verlag, New York, 1988).
[28] A. P. Levitt, *Whisker Technology* (Wiley-Interscience, New York, 1970).